

Ultrafast dynamics of periodic nanostructure formation on diamondlike carbon films irradiated with femtosecond laser pulses

Godai Miyaji^{a)} and Kenzo Miyazaki

Advanced Laser Science Research Section, Institute of Advanced Energy, Kyoto University, Gokasho, Uji, Kyoto 611-0011, Japan

(Received 3 July 2006; accepted 19 September 2006; published online 6 November 2006)

Using a pump-probe technique the authors have measured reflectivity of diamondlike carbon (DLC) film irradiated with femtosecond laser pulses to understand dynamic processes responsible for periodic nanostructure formation. The results have shown that characteristic reflectivity change observed as a function of superimposed laser shots is closely associated with the nanostructure formation and the bonding structure change to induce surface swelling, leading to a conclusion that the nanostructure formation on the DLC surface is certainly preceded by the bonding structure change. The nanoscale ablation to produce the nanostructure is discussed based on the local field generation on the surface. © 2006 American Institute of Physics. [DOI: 10.1063/1.2374858]

Laser-induced spatially periodic surface structures, so-called *ripples*, on solid materials have been studied extensively for more than two decades.^{1,2} The ripple structure formed with a linearly polarized laser field generally has a lateral period close to the laser wavelength λ , and the formation of this surface pattern has been explained by the interference between incident wave and surface scattered wave.^{1,2} In the recent experimental studies using femtosecond lasers, however, several groups have observed a new type of periodic structures with much smaller periods than the wavelength.^{3–10} In most cases, these subwavelength structures or nanostructures are produced at relatively low fluences of laser pulses. In fact, superimposed femtosecond laser pulses at fluences less than the single-pulse ablation threshold have produced the nanostructure with the period as small as $\sim\lambda/10$ or ~ 30 nm on hard thin films such as TiN and diamondlike carbon (DLC).^{4,11}

There has been a growing interest in these nanostructures, because they suggest a promising approach to nanoprocessing of materials with femtosecond lasers. It is well known, however, that the nanostructure formation with femtosecond laser pulses cannot be explained by the conventional ripple model, and thus the physical mechanism creating such nanostructures is an important subject to study.^{5–13} In the previous experiments for DLC films, Yasumaru *et al.*¹² and Miyazaki *et al.*¹³ have found that the nanostructure formation on the DLC surface is accompanied by the bonding structure change from DLC to glassy carbon (GC), and that the reflectivity change on the DLC surface is a good measure to monitor the experimental conditions to induce these morphological and bonding structure changes. These experiments suggested that the change in bonding structure may be a key to understanding the detailed process responsible for the nanostructure formation.

In this letter, we report the reflectivity measurement based on a pump-probe technique that was used to understand the ultrafast dynamics of the structural changes on the DLC surface. The results obtained have demonstrated that the nanostructure formation on the DLC surface is certainly preceded by the bonding structure change from DLC to GC,

since our measurements enabled us to resolve these two processes in the interaction.

DLC is an amorphous material consisting of a mixture of sp^3 diamond and sp^2 graphite structures. The thin DLC film of $1.6\ \mu\text{m}$ thickness used as the target was deposited on Si substrates. The surface roughness was measured to be ~ 15 nm with a scanning probe microscope (SPM). We used a Ti:sapphire laser system that produced 100 fs, 800 nm pulses at a repetition rate of 10 Hz. The output was split into two beams to produce a pump and a probe pulse. The pump pulse for ablation was focused in air at normal incidence onto the DLC surface, while the focused probe pulse was incident at the angle θ of 4° to measure the reflectivity R , as shown in the inset of Fig. 1(a). The pump focal spot was $230\ \mu\text{m}$ in diameter, and the laser fluence F was varied in a range of $F=0.06\text{--}0.2\ \text{J}/\text{cm}^2$. The pump fluence was less than the single-pulse ablation threshold of DLC, and the film surface was exposed to multiple pulses to induce ablation. The probe fluence was fixed at $0.2\ \text{mJ}/\text{cm}^2$, which was less than $1/300$ of the pump, so that the probe pulse never induced any structural change in the DLC film. The time delay Δt between the pump and probe pulses was controlled in the range of $\Delta t=0\text{--}70$ ps. The temporal and spatial overlap be-

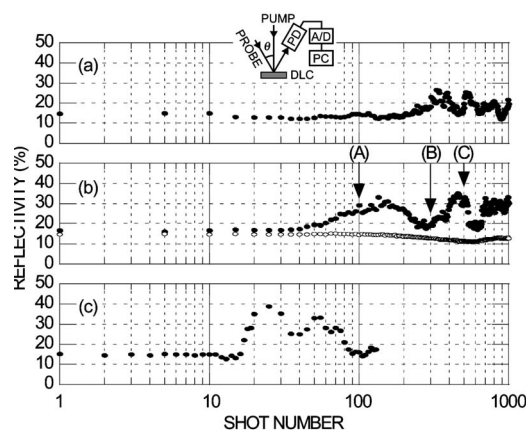


FIG. 1. Reflectivity measured with the probe pulses at $\Delta t=0$ as a function of N for (a) $F=0.12\ \text{J}/\text{cm}^2$, (b) $F=0.14\ \text{J}/\text{cm}^2$, and (c) $F=0.17\ \text{J}/\text{cm}^2$. The pump and probe polarizations are parallel for the solid circles and perpendicular for the white circles. The inset shows the irradiation and measurement geometry.

^{a)}Electronic mail: g-miyaji@iae.kyoto-u.ac.jp

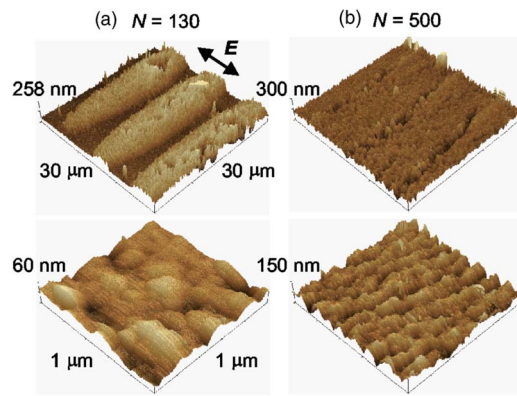


FIG. 2. (Color online) SPM images of the DLC surfaces irradiated with (a) $N=130$ and (b) $N=500$ at $F=0.14$ J/cm² and $\Delta t=0$ with the parallel polarizations. The upper image is for the central area of 30×30 μm^2 and the lower is for 1×1 μm^2 on the focal spot. The polarization direction is denoted with the arrows.

tween the pump and probe beams was confirmed by observing interference fringes on the target. The reflectivity R was defined by the ratio of the pulse energy detected in the direction at the angle of reflection, on the one hand, to the incident probe pulse energy, on the other hand, with calibrated p - i - n silicon photodiodes. The reflected probe pulse signal was converted shot by shot to the digital signal with a fast analog-to-digital converter and stored in a personal computer. The surface morphology was observed with the SPM, and the modification of bonding structure was analyzed with Raman spectroscopy using a 514.5 nm argon ion laser beam focused to the spot diameter of 10 μm at the sample surface.

Figure 1 shows typical examples of R measured at $\Delta t=0$ as a function of the number of laser pulses N for different fluences at which we have observed the nanostructure formation with superimposed laser pulses.¹³ Note that (1) the plot of R for parallel polarizations of the pump and probe beams shows two peaks as N increases and (2) the peak positions are shifted to smaller N as F increases.¹⁴ Such enhancement of the reflectivity R was never observed with the crossed polarizations, as shown in Fig. 1(b). In addition, at $\Delta t \geq 0.2$ ps we did not observe the enhancement of R even for the parallel polarizations. These results suggest that the enhancement of R observed is induced through a coherent interaction between the probe pulse and the DLC surface excited with the pump pulse. Furthermore, it is clear that the enhancement of R is induced by an incubation effect,^{13,15} whereby a portion of the pump energy is accumulated in the target material, since the pump fluence used is less than the single-pulse ablation threshold.

The observed characteristic changes in R have provided a clue to the interaction process on the target surface. To see the correlation between the changes in R and the surface morphology, we observed the DLC surfaces with the SPM. Figure 2 shows the images of the DLC surface irradiated with (a) $N=130$ and (b) 500 at $F=0.14$ J/cm², where R is peaked as seen in Fig. 1(b). In Fig. 2(a), the upper image represents an interference pattern formed by the pump and probe beams in the focal area, while no ablation to produce the nanostructure is induced, as seen in the lower. The spacing between fringe peaks or crests is measured to be $L \sim 11$ μm with the averaged height of ~ 100 nm, which corresponds to $L=\lambda/\sin \theta$ with $\lambda=800$ nm and the angle $\theta=4^\circ$ between the pump and the probe beams. Scanning the probe

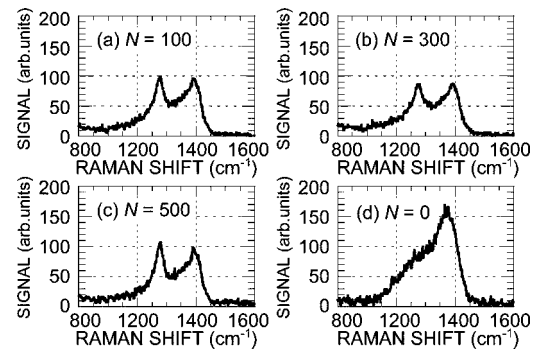


FIG. 3. Raman spectra of DLC surfaces irradiated with (a) $N=100$, (b) $N=300$, and (c) $N=500$ at $F=0.14$ J/cm², together with (d) the spectrum of nonirradiated DLC. The experimental conditions for (a), (b), and (c) are the same as those at (A), (B), and (C) in Fig. 1(b).

microscope over a broad area, we have found that this grating structure was formed due to swelling of the irradiated DLC surface. In the femtosecond laser ablation experiments, such swelling of DLC surface has been observed to result from the mass density change due to the modification from DLC to GC or graphite.^{16,17} With an increase in N , the grating groove is observed to become shallow due to ablation initiated at the crest, while the nanostructure starts to be formed on the crest, as seen in Fig. 2(b).

When the grating is formed on the surface, the pump pulse can partially be diffracted into the direction of the reflected probe beam to increase R . We could measure the diffraction efficiency of $\sim 0.5\%$ for the surface shown in Fig. 2(a). This diffraction leads to an increase in R by about 20%, which is in good agreement with $R \sim 33\%$, as observed in Fig. 1(b). The diffracted pump wave was also detected in the backward direction with respect to the incident probe pulse. These results demonstrate that the enhanced R in Fig. 1 is certainly due to the grating formation on the DLC surface.

As mentioned above, the swelling that forms the grating on the DLC film should be due to the change in bonding structure of DLC layer. We confirmed this by the Raman spectra of an initially swelled fringe on the surface. Figure 3 shows the results for (a) $N=100$, (b) $N=300$, and (c) $N=500$ at $F=0.14$ J/cm², together with the spectrum of (d) nonirradiated DLC for comparison, where each in (a), (b), and (c) corresponds to the spectrum for the target marked as (A), (B), and (C) in Fig. 1(b). In contrast to the DLC spectrum having a single broad peak at 1530 cm⁻¹, those in (a), (b), and (c) include two peaks at 1355 and 1590 cm⁻¹. The two peaks in a spectrum started to be observed with an increase in R , representing the structural change from DLC to GC.^{12,13} We note that, as shown in Fig. 3(a), this structural change is induced with $N \sim 100$ around the first peak of R in Fig. 1(b), where neither ablation nor nanostructure formation is induced yet, as shown in Fig. 2(a). In Fig. 3(b) the spectral peaks become smaller than those in Fig. 3(a). This suggests that the partial content of GC in the surface layer is decreased at $N \sim 300$, where R is almost minimized, as seen in Fig. 1(b). The most distinct GC spectrum having the larger peak at 1355 cm⁻¹ than at 1590 cm⁻¹ is observed at $N \sim 500$, as shown in Fig. 3(c), where the second peak of R appears in Fig. 1(b). These results show that the characteristic change of R is closely related to the morphological and bonding structure changes on the film surface. To see it in detail, we measured the mean spacing l and depth d of the

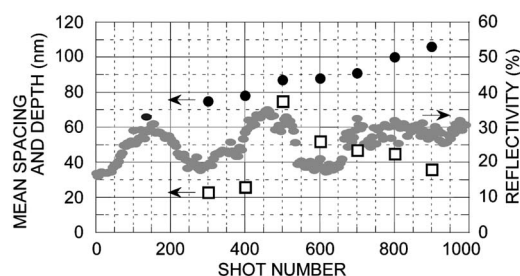


FIG. 4. Mean spacing (circles) and depth (white squares) of periodic nanostructures measured with the SPM as a function of N for the DLC irradiated under the same conditions as in Fig. 1(b). The gray circles represent the same data points of R for the parallel polarizations as in Fig. 1(b).

nanostructure produced on the initially swelled fringe. The result measured as a function of N at $F=0.14 \text{ J/cm}^2$ is shown in Fig. 4. The periodic nanostructures with $l=80\text{--}110 \text{ nm}$ are observed in the range of $N=300\text{--}900$. We note that the observable nanostructure starts at $N\sim 300$, where R decreases down to a minimum after the first peak. With an increase in N , the structure depth d increases to the maximum at $N\sim 500$, where R increases up again to the second peak. Blocking off the probe pulses we have confirmed that the nanostructure was certainly formed with the pump pulses.

Referring to the result of R shown in Fig. 1(b) or 4, we will discuss the interaction dynamics for the structural changes on the DLC surface. With increasing N , the femto-second laser pulses first induce the surface modification from DLC to GC. This change is induced by the selective transition from the sp^3 bonds in DLC to the sp^2 for GC, due most likely to the sp^3 dissociation energy smaller than the sp^2 . The pump pulse energy is partially stored in the thin film through the bonding structure change, and then the structural change is accumulated and detected as the surface swelling to form the grating at $N\sim 130$, as seen in Fig. 2(a).

With a further increase in N , the measurable nanostructure is formed with $N\sim 300$, as shown in Fig. 4, indicating that the nanoscale ablation responsible for the formation of the nanostructure should be initiated locally before that, i.e., at $N<300$. Since no ablation is observed around $N\sim 130$, the decrease in R after the first peak in the region of $\sim 130 < N < 300$ is due to the local ablation on the swelled surface. This is consistent with the fact that the sp^2 bonds would preferentially be ionized with the femtosecond laser pulses due to the lower ionization energy (or band gap) than that of the sp^3 . Thus, we may conclude that the change in the bonding structure from DLC to GC certainly precedes the ablation to form the nanostructure.

The initiation of local ablation on the swelled surface should lower the GC volume and resulting diffraction efficiency or R , as seen in Fig. 1(b) or 4. With a further increase in N to $300 < N$, the measured N -dependent R suggests that the change from sp^3 to sp^2 bonds would grow again in the ablated area. This leads to an increase in ablation that subsequently reverses the crest and trough of the initial grating, while the trough would continuously swell due to the incident pump field. In fact, we have observed such a reversed structure of the grating at $\sim 400 < N$. With $N\sim 500$, the deepest nanostructure is formed, where the second peak of R is observed as seen in Fig. 4, as well as the clear change from

DLC to GC for the initial crest on the surface, as shown in Fig. 3(c). Thus, the preferential change in the bonding structure would keep alternating between crests and troughs with increasing N until the original DLC layer is completely removed.

The present experiment also demonstrates that a small modulation of the laser field created by the weak probe pulse with a fluence of about $1/700$ of the pump has produced a large morphological change or the grating through the accumulation of bonding structure changes, as shown in Fig. 2(a). This implies that we may assume the generation of weak local field to form the nanostructure. As discussed above, the bonding structure change before the ablation increases the efficiency of free-electron generation in the DLC surface. The free-electron density would not be uniform, due most likely to the initial surface roughness smaller than the wavelength, as seen in the lower image of Fig. 2(a). The nonuniform free-electron density is able to create a local field modulated on a nanometer scale¹⁸ that initiates the nanoscale ablation.

In summary, using the pump and probe technique we have investigated the reflectivity change to understand the interaction dynamics for the modification from DLC to GC and the nanostructure formation. Our measurements have resolved the ultrafast evolution from the former to the latter and demonstrated that the nanostructure formation on the DLC surface is certainly preceded by the change in the bonding structure from DLC to GC. The results obtained suggest that the generation of local field plays a major role in the nanostructure formation.

The authors thank A. E. Kaplan for his discussion and W. Kobayashi, N. Yasumaru, and J. Kiuchi for their support in the initial experiment.

¹Z. Guosheng, P. M. Fauchet, and A. E. Siegman, Phys. Rev. B **26**, 5366 (1982).

²J. Wang and C. Guo, Appl. Phys. Lett. **87**, 251914 (2005).

³J. Reif, F. Costache, M. Henyk, and S. V. Pandelov, Appl. Surf. Sci. **197-198**, 891 (2002).

⁴N. Yasumaru, K. Miyazaki, and J. Kiuchi, Appl. Phys. A: Mater. Sci. Process. **76**, 983 (2003).

⁵Q. Wu, Y. Ma, R. Fang, Y. Liao, Q. Yu, X. Chen, and K. Wang, Appl. Phys. Lett. **82**, 1703 (2003).

⁶A. Borowiec and H. K. Haugen, Appl. Phys. Lett. **82**, 4462 (2003).

⁷Y. Dong and P. Molian, Appl. Phys. Lett. **84**, 10 (2004).

⁸P. Rudolph and W. Kautek, Thin Solid Films **453-454**, 537 (2004).

⁹J. Bonse, M. Munz, and H. Sturm, J. Appl. Phys. **97**, 013538 (2005).

¹⁰T. Tomita, K. Kinoshita, S. Matsuo, and S. Hashimoto, Jpn. J. Appl. Phys., Part 2 **45**, L444 (2006).

¹¹N. Yasumaru, K. Miyazaki, and J. Kiuchi, Appl. Phys. A: Mater. Sci. Process. **81**, 933 (2005).

¹²N. Yasumaru, K. Miyazaki, and J. Kiuchi, Appl. Phys. A: Mater. Sci. Process. **79**, 425 (2004).

¹³K. Miyazaki, N. Maekawa, W. Kobayashi, M. Kaku, N. Yasumaru, and J. Kiuchi, Appl. Phys. A: Mater. Sci. Process. **80**, 17 (2005).

¹⁴At $F=0.17 \text{ J/cm}^2$ we observed complete removal of the DLC layer from the central focal area with $N\sim 100$, where the measurement was stopped.

¹⁵J. Bonse, P. Rudolph, J. Krüger, S. Baudach, and W. Kautek, Appl. Surf. Sci. **154-155**, 659 (2000).

¹⁶N. Yasumaru, K. Miyazaki, J. Kiuchi, and H. Magara, Proc. SPIE **5662**, 755 (2004).

¹⁷T. V. Kononenko, V. V. Kononenko, S. M. Pimenov, E. V. Zavedeev, V. I. Konov, V. Romano, and G. Dumitru, Diamond Relat. Mater. **14**, 1368 (2005).

¹⁸S. I. Bozhevolnyi, in *Optics of Nanostructured Materials*, edited by V. A. Markel and T. F. George (Wiley, New York, 2001), Chap. 3.